COMPOSITION, STRUCTURE AND PHYSICAL PROPERTIES OF FOETAL CALF SKIN

M.Ventre[1], M.Padovani[2], A.D.Covington[2], P.A.Netti[1]

[1] Department of Materials and Production Engineering University of Naples Federico II 80125, Naples, Italy
[2] British School of Leather Technology, University of Northampton; Boughton Green Road
NN2 7AL Northampton, United Kingdom

Abstract

In the present study a characterisation of structure, composition and mechanical properties of foetal calf leather is reported. In order to evaluate tissue development over maturation, a comparison has been made between foetal calf and adult bovine leather properties. A comparison of results from the present and studies already present in literature has yielded novel observations concerning the relationship between skin mechanics, composition and microarchitecture during maturation.

Structural and morphological analyses have been carried out with electron microscopy and optical microscopy. Mechanical properties were determined according to traction testing. Differential scanning calorimetry, as well as hydrothermal isometric tension were undertaken in order to evaluate thermal properties. Chemical assays, such as 4-hydroxyproline and elastin content, have been used to quantify tissue composition.

Scanning electron micrograph, and histochemical analysis of leather cross sections revealed the existence of gradients in terms of structure and composition. In particular the grain appears like a compact network of thin collagen fibres and rich in elastin while the corium is an entangled mass of collagen bundles. This peculiar architecture provides the tissue with non linear and highly anisotropic mechanical properties. Moreover traction tests demonstrated that such mechanical properties are strongly dependent on sampling position, suggesting that collagen fibres seeding in a specific texture is already evident in the foetal stage and does not necessary require any mechanical training. Differential scanning calorimetry and hydrothermal isometric tension supplied useful information on crosslinks density and their thermal stability. The correlation of these data suggest that the improved mechanical properties exhibited by mature tissues have to be ascribed to the higher crosslink density rather than collagen content, which remains basically constant during the development.

Introduction

Skin is a biochemically and biomechanically complex connective tissue. Skin macroscopic physical properties are strongly related to its biochemical composition and the spatial arrangement of the microconstituents. Mature bovine skin has been widely studied and correlation between relative composition and mechanical properties has already been published. However, it is still unclear how developmental changes (matrix remodelling and maturation) can affect macroscopic properties. As examples, collagen crosslinks undergo extensive changes in terms of chemical structure and concentration with age; immature elastic microfibrils are crosslinked and enriched with amorphous elastin. A comparative study on foetal and mature skin has been undertaken in order to gain data skin mechanical properties and on elastin content and its distribution in the dermal layer. Moreover, in order to achieve information on collagen fibre bundles configuration, mechanical tests have been carried out on a partially processed leather (skin almost devoid of non collagenous proteins). This work endeavours to determine a relationship between tissue composition, structure and physical properties and shows that skin possesses highly anisotropic mechanical properties and its microconstituents are not uniformly spread all over its thickness.

Materials and methods

Tensile strength tests – foetal skin and leather

Tensile tests were carried out on nine (C, I, M, N, Q, R, T, U and Z) soaked skin samples and chrome tanned leather. Tanning process details are reported in the Annexes I. The specimens were taken from the official sampling area, provided by the ISO2419 standard, both along the backbone direction and in the orthogonal direction. Shape and dimensions of the specimens are shown in Fig. 1.

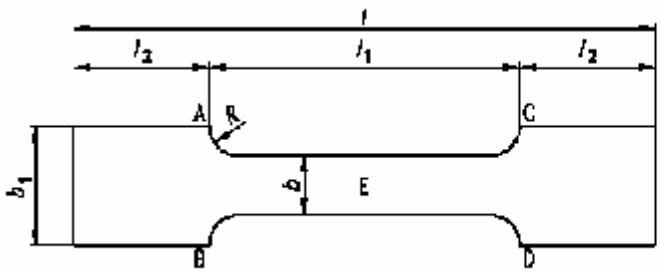

Fig. 1 Specimen shape for tensile testing bovine hide

Designation	Measure [mm]
l	40
l_1	20
L_2	10
b	4
b_1	9.3

Table1 Specimen dimensions for tensile testing foetal skin

Tests were carried out using a Stable Micro Systems testing machine at crosshead speed of 40 mm/min.

Foetal calf skin samples were soaked in distilled water for 24 hours at 4°C prior testing.

Chrome tanned leather were stored in the conditioning room (60% humidity and 23°C) for at least 24 hours prior testing.

Tensile strength tests – bovine skin

Tensile tests were carried out on one (sample bov) adult bovine hide. The specimens were taken from the official sampling area, provided by the ISO2419 standard, both along the

backbone direction and in the orthogonal direction. Specimen dimensions are reported in the Table 2.

Designation	Measure [mm]
l	110
l_1	50
l_2	30
b	10
b_1	25

Table 2 Specimen dimensions for tensile tests on bovine hide

Tests were carried out using a Stable Micro Systems testing machine at crosshead speed of 40 mm/min.

Differential Scanning Calorimetry

Eight foetal calf skins (Samples C, I, M, N, Q, T, U and Z) and one (sample bov) bovine skin samples were unhaired and defleshed with a surgical scalpel. Each sample was soaked in twice distilled water for 48h at 4°C. Water was changed every 12h. Surface water was removed prior to testing.

Nine foetal calf chrome tanned leathers were stored in a conditioning room (60% humidity and 23°C) for at least 24 hours prior to testing. DSC analysis was performed with a Mettler-Toledo model DSC822e.

The temperature program consisted of a ramp from – 40°C up to 80°C at a heating rate of 10 °Cmin^{-1}. Each experiment was carried out in triplicate

Hydrothermal Isometric Tension

Seven (Sample C, I, Q, R, T, U and Z) foetal calf skin samples and one (Sample bov) bovine skin samples were cut in the shape shown in fig 1. One foetal calf sample (Sample R) was treated with sodium borohydride ($NaBH_4$) in borate buffer pH 9 at 0°C for 90 minutes. These samples were also taken from the official sampling position standard. The HIT test consists of monitoring the stress produced by collagenous tissue while it is heated above its shrinkage temperature. Each sample was positioned between the jaws, with an initial load of 50g. It was equilibrated in distilled water at room temperature for 30 minutes prior to testing. The bath was heated up to 85°C (heating rate 2°Cmin^{-1}) and then the temperature was kept constant for 2 hours. Each experiment was carried out in triplicate.

Stepwise HIT test

This was applied to one sample of foetal calf skin (sample R). Three specimens were processed with $NaBH_4$ (borate buffer pH 9 at 0°C for 90 min). The rationale of the test is analogous to the HIT test. The only difference is that the heating is a step function with 5°C amplitude increase and 75 min intervals. The starting and final temperatures were set at 60°C and 85°C respectively.

Scanning Electron Microscopy

SEM examinations were carried out using a Hitachi S-3000N SEM.

Total Collagen determination

The total collagen content in the tissue was determined by following a spectrophotometric procedure developed and reported by Jamall et al. [1]. 400mg of unhaired fresh foetal calf skin were placed in a digest tube with 5ml of HCl 37% and left overnight in oven at 100°C. After complete digestion the solution was neutralised with concentrated sodium hydroxide solution and the volume made up to 10ml.

0.55ml of this solution were added to a solution of 1.27ml of diluent (2-propanol:water, 2:1) and Choramine T and then were left to react at room temperature for 10 min. After the reaction, 2.3 ml of Ehrlichs reagent (0.6 M DMAB in 50ml of 2-propanol and 9ml $HClO_4$) were added and the solution was left to react for 10 min at 70°C. Spectrophotometric readings were taken at 555nm and the unknown concentration was extrapolated from a standard curve obtained using a standard solution (0.100g/l) of L-hydroxyproline at different concentrations.

Elastin determination

Elastin was extracted from foetal and adult bovine skin using the Fastin Elastin Assay provided by Biocolor Ltd.

Spectrophotometric readings were taken at 513nm and the unknown concentration was extrapolated from the standard curve obtained using a standard solution (1mg/ml) of elastin at different concentrations.

Results

Collagen content

The collagen contents of the analysed skins are given in Table 3.

Skin samples	mg of collagen /gram of skin	% collagen
foetal skin s	206	20.6
foetal skin p	244	24.4
foetal skin d	170	17.0
foetal skin f	270	27.0
Adult bovine 1	207	20.7
Adult bovine 2	216	21.6

Table 3 Collagen concentration in wet tissue

Elastin content

Elastin content of foetal and mature skins is reported in Table 4.

Skin samples	mg/g of wet skin	% for 1g of wet skin
foetal skin s	1.36	0.14
foetal skin p	1.66	0.17
foetal skin d	0.56	0.06
foetal skin f	1.57	0.16
Adult bovine 1	9.68	1
Adult bovine 2	9.51	1

Table 4 Elastin concentration in wet tissues

Static traction testing

Typical stress-strain diagram for both soaked skin and leather is shown in Fig. 2.

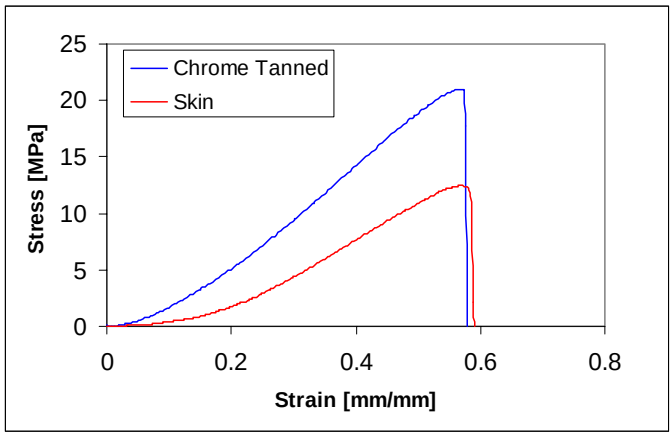

Fig. 2 Sample N stress-strain plot for skin and leather

The tangent at the origin will in the following be referred to as the starting modulus, while the slope of the linear region is the linear modulus. The part of the diagram before the linear region is usually referred to as the *toe region*.

In Table 5 and Table 6 the values of elongation at break, ultimate tensile strength, linear modulus, for soaked skin and leather respectively are summarised.

Sample	Elongation at break [%]		Ultimate tensile strenght [MPa]		Modulus	
	AVG	ST. DEV.	AVG	ST. DEV.	AVG	ST. DEV.
C	62.47	5.54	16.45	0.39	47.88	4.33
I	55.87	3.83	20.55	0.72	59.69	6.52
M	49.07	1.50	16.74	0.19	51.86	0.97
N	63.88	6.62	12.89	0.30	33.65	5.67
Q	57.76	4.15	16.60	1.22	47.54	3.64
T	54.94	1.46	17.70	0.43	50.84	2.27
U	66.37	5.69	16.84	1.40	51.13	7.51
Z	62.00	5.75	20.61	3.04	58.29	6.72

Table 5 Skin mechanical properties

Sample	Elongation at break [%]		Ultimate tensile strenght [MPa]		Modulus	
	AVG	ST. DEV.	AVG	ST. DEV.	AVG	ST. DEV.
C	53.29	2.45	38.42	3.65	88.07	12.09
I	61.32	0.90	33.91	0.86	79.85	2.95
M	55.55	2.39	40.71	3.00	75.10	10.83
N	62.96	4.00	29.94	2.24	61.50	5.92
Q	43.03	2.67	46.86	2.81	107.04	16.38
T	71.34	2.27	30.51	1.36	73.03	3.00
U	46.00	3.44	31.23	3.13	95.71	6.96
Z	50.22	2.67	33.51	1.66	96.53	4.26

Table 6 Leather mechanical properties

Dynamic traction tests

The applied load cycles produce the set of curves depicted in Fig. 3.

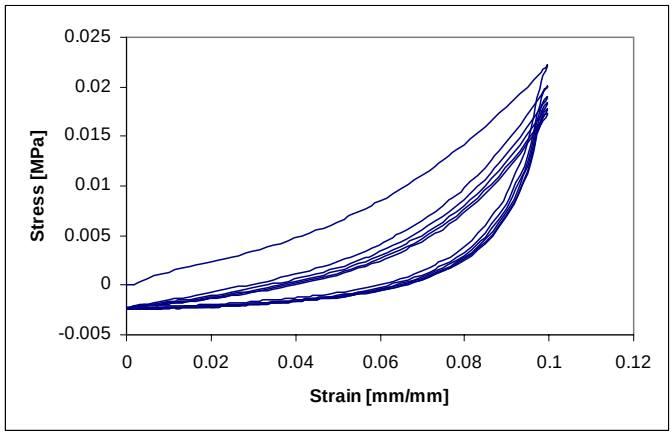

Fig. 3 Sample F: dynamic stress-strain plot

Parameters of interest are the starting modulus and the energy loss between two adjacent cycles (area bounded between load and unload). The evolution of both modulus and energy as a function of will be evaluated cycles in the following sections.

Differential scanning calorimetry

Thermograms of samples C, U, Z and bovine are shown in Fig. 4 and the numerical values of onset temperature and peak temperature for all the samples tested are shown in Table 7.

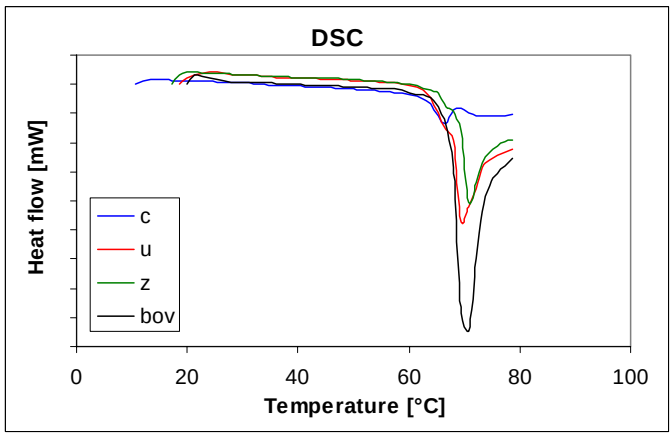

Fig. 4 Sample C, U, Z and mature skin average DSC thermograms

	Peak [°C]		Onset [°C]	
	AVG.	ST. DEV.	AVG.	ST. DEV.
C	66.06	0.09	63.46	0.14
I	67.34	0.47	64.08	0.22
M	66.66	0.44	63.48	0.19
N	67.00	0.13	63.79	0.56
Q	65.47	1.08	63.19	1.63
T	65.80	0.03	63.30	0.80
U	68.57	0.30	64.00	0.15
Z	69.83	0.40	65.18	0.46
bovine	69.22	0.04	67.03	0.20

Table 7 Skin thermal properties evaluated with DSC experiments

Hydrothermal Isometric Tension
A typical HIT diagram is shown in Fig. 5.

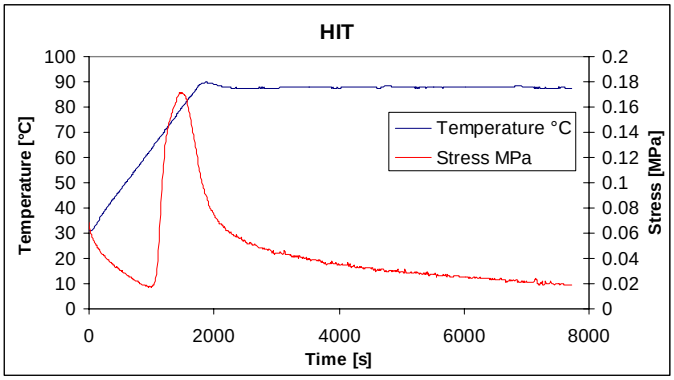

Fig. 5 Sample U HIT profile

Stress and temperature are linked by the variable time. It is therefore more convenient to plot stress as a function of temperature.

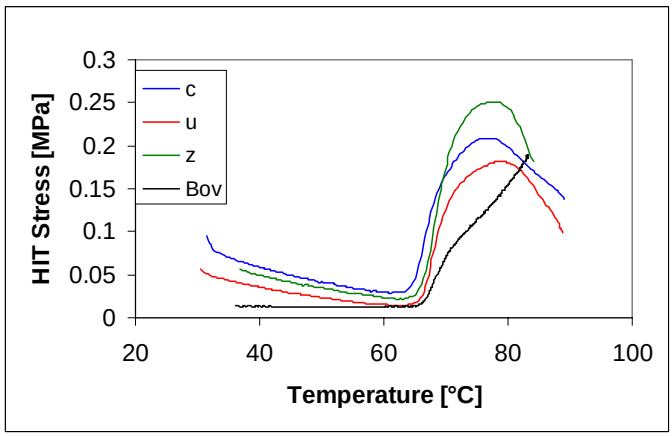

Fig. 6 Samples C, U, Z and mature skin: stress-temperature plot

Discussion

For both skin and chrome tanned leather the mechanical behaviour is non linear: at lower strain (i.e. low stress) the slope of the curve is shallow. For higher strain, the stress strain response becomes nearly linear. The mechanism which determines the properties of the first part of the curves is collagen fibres unravelling and their alignment toward the applied load. The more aligned are the fibres shorter is the first part of the diagram. Such a mechanism is known as *fibre recruitment.*

The deformation mechanism of leather at low strain values has been studied by Wright *et al.* [2]. They have suggested that, on a microscopic scale, the dominant mode of deformation is fibril flexure rather than individual fibril stretching. For collagenous tissues, a non-affine deformation mechanism has been demonstrated, which is assumed to arise from the composite nature of biological tissue [3]. In particular the non-affine fibre behaviour in pig skin has been attributed to a non-affine relationship between the collagen and the ground substance [4]. However leather is not a truly composite material, since almost all the non-structural proteins are removed during the tanning process. For such material, affine

deformation hypothesis could be still applied [5]. If the data depicted in Fig. 2 are plotted in terms of displacement and load, it appears that the natural tissue is somehow the strongest (Fig. 7).

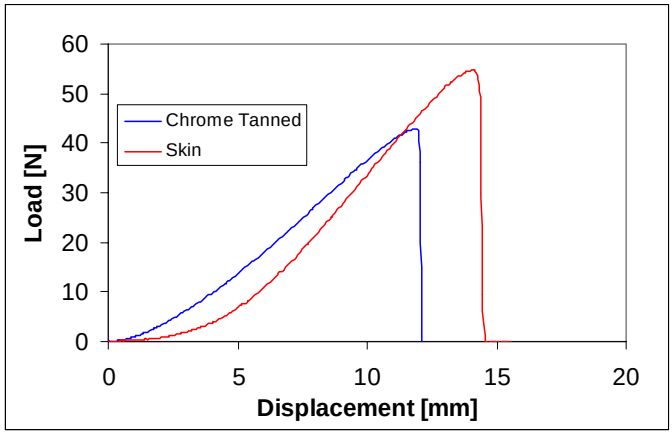

Fig. 7 Sample N load-displacement plot

The differences in the two figures have to be assigned to the difference in the cross sectional area of the two materials. The swollen skin cross sectional area is greater than the leather one. The load bearing fibres concentration is then decreased in the natural tissue in a water swollen state, i.e. a smaller value of the tensile stress, in terms of MPa, is attained dividing the load by a larger cross section. The presence of a liquid phase among collagen fibres also affects the mechanical properties in the toe region: aqueous solution could push the fibres apart increasing the so called “angle of weave” and therefore the recruitment process is delayed; moreover its lubricant action could decrease the load transfer. During the tanning process the natural tissue is damaged up to a certain extent and such weakening effect it is not balanced by the action of chromium, which does not act as a mechanical crosslink[6].

Skin, as well as leather, is an anisotropic material. Mechanical properties are strongly dependent on the sampling position and the direction of applied load, as it shown in Fig. 8, where the stress-strain response of the one foetal leather in two mutually orthogonal direction of applied load is reported.

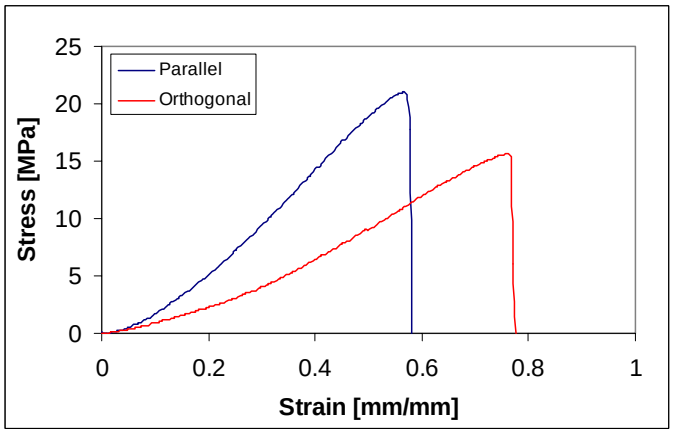

Fig. 8 Sample N stress-strain plot in two mutually orthogonal direction of applied load

The recruitment phase is delayed, suggesting that the collagen bundles have been seeded, even in the foetal stage, in a preferential direction. Linear modulus is significantly different

which states that different amount of fibre bundles are involved during the deformation mechanism.

Mechanical behaviour is dramatically affected by the sampling position. Foetal calf skins are small (less than $1m^2$) and physical properties between two adjacent parts can be significantly different. Results of mechanical tests are always a compromise between having a statistically significant number of specimens to test and testing comparable materials, since leather is locally non-uniform to a considerable degree [7]. As an example, samples taken away from different zones of chrome tanned foetal calf leather Sample H have been tested, in the same way as described above. Details on the sampling position are shown in fig. 9 and Table 8.

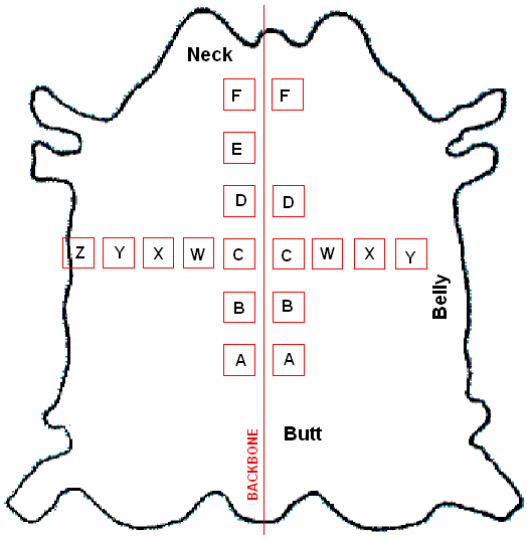

fig. 9 Sample H sampling position schematic

	Left hand side		Right hand side	
Position	Distance from the neck [cm]	Distance from the backbone axis [cm]	Distance from the neck [cm]	Distance from the backbone axis [cm]
A	60	3.5	60	4
B	50	4	50	5
C	40	5	40	5.5
D	30	4.5	30	5.5
E	20	5	-	-
F	10	5	10	6
W	40	11.5	40	12
X	40	17	40	18
Y	40	22	40	23
Z	40	28	-	-

Table 8 Sample H sampling position distances

The values of the modulus in both the directions parallel and perpendicular to the backbone, are shown in the following bar diagrams.

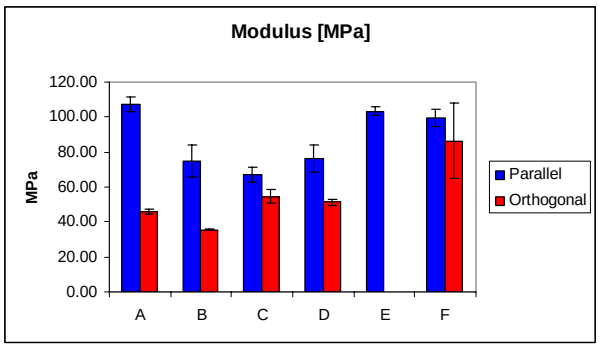

Fig. 10 Sample H linear modulus along the backbone

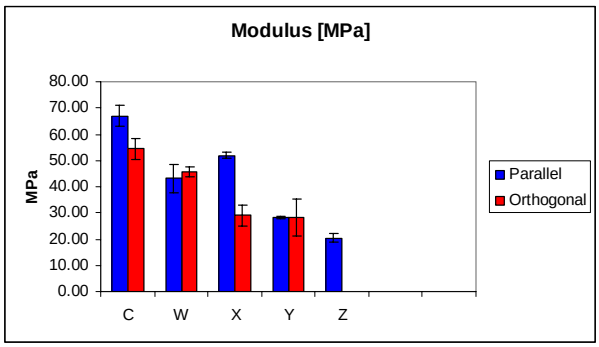

Fig. 11 Sample H linear modulus across the backbone

Fig. 10 suggests that, following the backbone length, the collagen fibres in position A and E posses higher modulus; and those fibres are in proximity of the pelvic and thoracic girdle respectively. Osaki suggests that collagen fibres in skin are mostly aligned in the direction parallel to the back bone and limbs. This direction corresponds to the direction “perpendicular to that of skin motions accompanied with muscular motions in the abdomen and hindlimbs due to eating and walking, and that the degree of orientation was large in the parts where the skin motions are marked” [7]. Moving away from the back bone (Fig. 11) the fibres become softer and softer. Samples with comparable values of both moduli (positions F, W and Y) probably are made: 1. of fibres prevalently aligned in a direction tilted of 45° respect the backbone axis; 2. the material itself is planar isotropic.

These results indicate the anisotropic behaviour in the plane of skin. The anisotropy arises from a fibre preferential spatial arrangement within the structure, i.e. there exists a prevalent population of fibre bundles disposed in the same parallel direction. However, electron micrographs clearly show that the skin (as well as leather) cross section possesses structural heterogeneities as shown in Fig. 12.

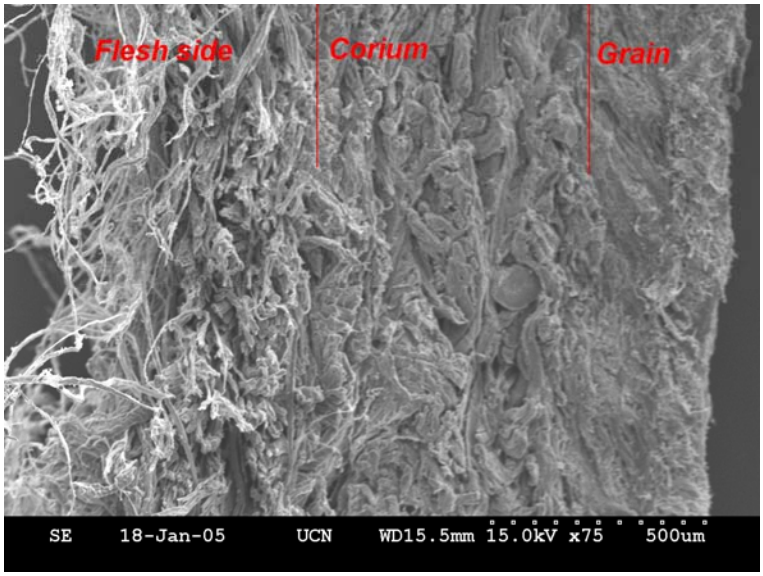

Fig. 12 Scanning eldectron photomicrograph of a foetal calf leather

Dermis multilayered structure here depicted is evident: the corium layer is an entangled mass of thick bundles and the grain, composed of a network of thin fibres.

Besides structural heterogeneity, ECM composition presents gradient throughout the thickness. The elastic network is an example, as it is confirmed by the optical micrograph of a foetal calf cross section stained with orcein red, shown in Fig. 13.

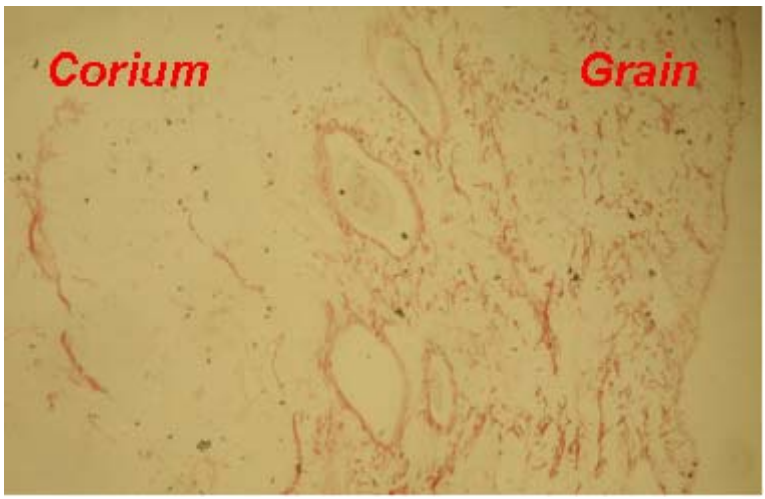

Fig. 13 Histochemical stain for foetal elastin network

As it is shown, the elastin is not spread all over the leather thickness, but it is present in the grain side and all around the hair follicules. Since the elastin content in skin is modest and owing to its weak mechanical behaviour [8] it is unlike to affect the static properties of both leather and skin.

In Fig. 14, the starting modulus is plotted against dermal elastin content. It seems that a correlation exists between the two parameter, i.e. a tenfold increase of the elastin content produces almost a fourfold increase of the starting modulus.

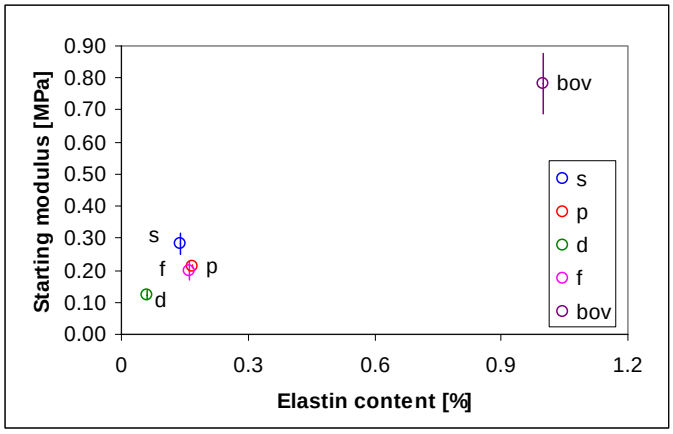

Fig. 14 Starting moduls – elastin content plot

It is unlikely that the elastic network is the only factor responsible for the early tissue mechanical response. Bending stiffness of mature collagen fibre bundles, as well as interaction between the ground substance and the fibre network could play non negligible effects. During the foetal stage, however, collagen bundles are thinner and microfibrillar in nature as confirmed in the following two electron photomicrographs.

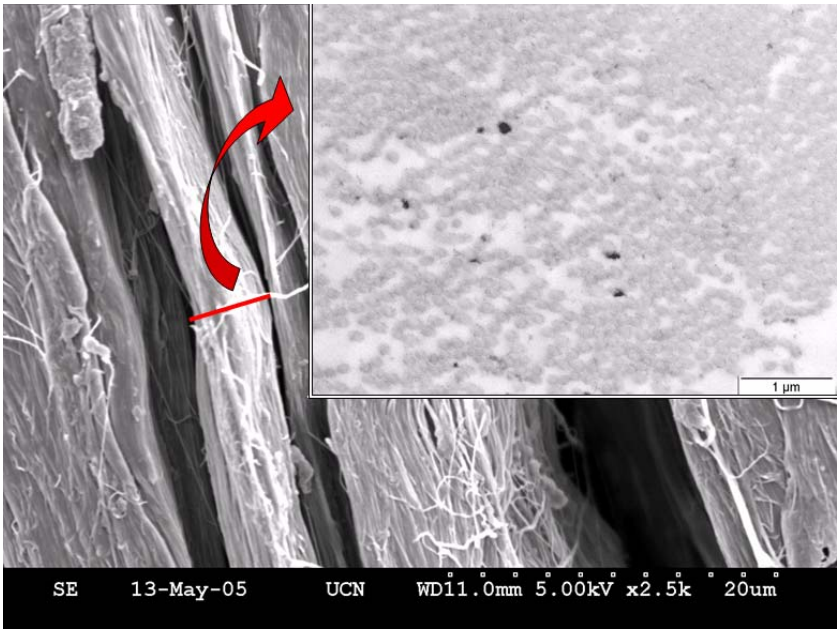

Fig. 15 Scanning electron micrograph of foetal calf leather. Top right: Transmission electron photomicrograph of a foetal collagen bundle

It may be assumed then, that the collagen boundless bending stiffness is negligible, or, at least, it roughly induces comparable effects for all the foetal skin tested. Thus the relative influence of the elastic network on early tissue mechanic response is higher and this assumption could explain the correlation between elastin content and starting modulus in the foetal stage. Moreover, elastin network could have a role in collagen bundle recoil. In Fig. 16, histograms of the energy loss in cyclic testing are reported.

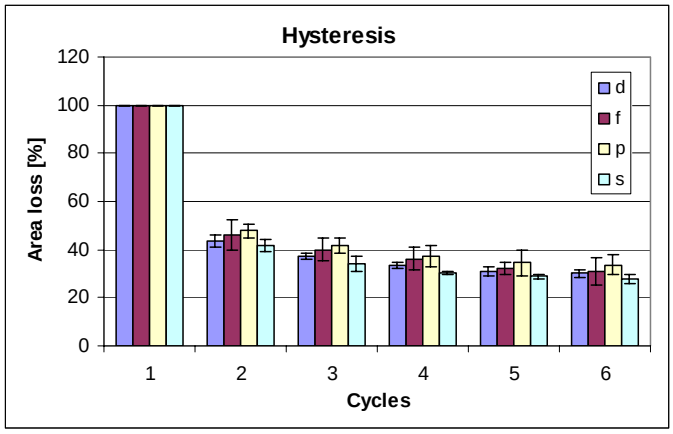

Fig. 16 Percentage area loss in dynamic test

The *i-th* percentage area loss here refers to the difference in the area enclosed between loading and unloading curves between the *i-th* cycle and the first cycle. Ideally, area zero would mean a perfectly elastic (non-linear) material, while a constant hysteresis value means that the material involves the same amount of energy for the deformation cycle. Sample P, which is characterised by a higher value of elastin, damps less energy (hysteresis remains almost constant during cycles, with slightly higher average value). Sample S dissipates more energy, even though has the highest value of starting modulus. This inconsistent behaviour might be explained by monitoring the evolution of its starting modulus during cycles.

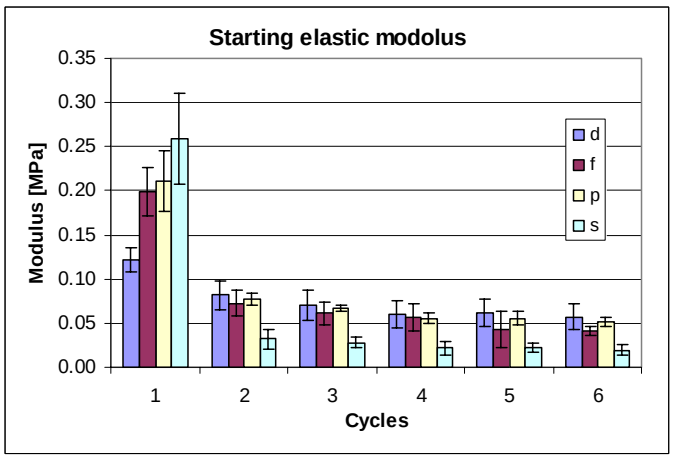

Fig. 17 Starting modulus evolution in dynamic test

As shown in Fig. 17, there is a dramatic modulus drop. This means that the material is severely damaged after the first cycle and such damage could explain the energy loss value. Probably other interfibrillar proteins (or proteoglycans, hyaluronic acid) confer the tissue with higher starting stiffness. After the first cycle, this interfibrillary network is completely broken down and is not able to withstand the load anymore.

As stated earlier, elastin content does not seem to influence linear modulus values whatsoever. Linear modulus value strictly depends on the stretching of collagen fibre bundles. In particular, it is acknowledged that collagen crosslinking density influences collagen fibre stiffness. In order to gather information on the amount and nature of the crosslinks present in the tested tissues, calorimetric analysis have been carried out. Covalent crosslinks not only provide the tissue with mechanical strength, but also confer thermal stability. As a

consequence of that, thermal analyses are an indirect method for crosslink density quantification.

Collagen thermal denaturation occurs around 60-70°C, where DSC thermograms exhibit an endothermic peak. In the temperature range mentioned above, the thermal energy is enough high to allow the collagen triple helix – random coil transition.

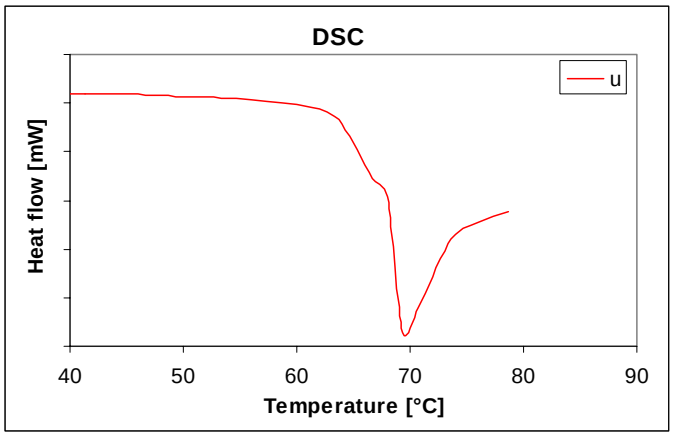

Fig. 18 Sample U magnification of the DSC thermogram

It is supposed that the mechanism of uncoupling of the three α-chains starts in a particular region of the triple helix, called the *thermally labile domain* [9]. This domain is identified in a hydroxyproline free sequence, 65 residues long, nearby the C terminus.

According to the "polymer-in-a-box" model, Miles *et al.* [10] have explained the mechanism of collagen thermal denaturation and the influence of hydration on the thermal stability of collagen. This model assumes the collagen triple helix bounded in a box, which is the volume available between this molecule and the molecules surrounding.

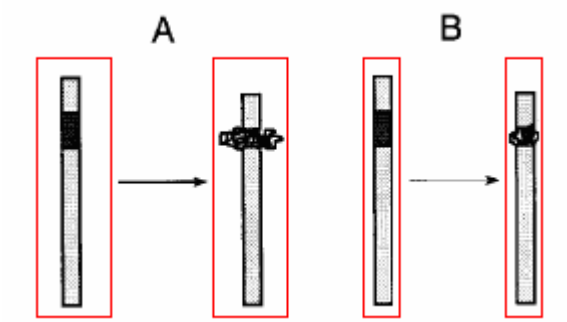

Fig. 19 Schematic of the polymer-in-a-box model (from Miles *et al.* [10]modified)

As shown in Fig. 19, reducing lateral dimension of the box, by dehydration, will reduce the configurational entropy of activation of the uncoupling of the thermally labile domain and thereby will increase the Gibbs free energy of activation and consequently will stabilise the whole structure. Such a model explains why individual collagen molecules and collagen fibres swollen in acidic solution possess lower denaturation temperature: in both cases the box dimensions are larger in relation to the collagen molecules and the box itself is no longer a constraint for the lateral expansion of the thermally labile domain. For the same reason, collagen present in highly packed structures, such as tendons and ligaments, are very stable. It should be noted that, in fibrils, the thermally labile domain is situated in the gap zone where it

has enough space to expand laterally on thermal activation. It is therefore probable that thermal labile domain of the molecule in solution in the same region of the molecule in the fibre and is the region responsible for the collagen instability.

The collagen denaturation peak reported in Fig. 18 is strongly asymmetric and non-regularly shaped. A shoulder is usually present 3–5°C before the main peak, especially for immature tissues. Sometimes such a shoulder degenerates into an adjacent and smaller peak. These observations suggest that collagen is present in foetal skin in ordered structures, such as fibres and fibre bundles and in oligomers like dimers, trimers, and so on. As stated earlier, accordingly to the polymer in a box model, collagen triple helices inside fibrils and fibres, are more stable than triple helices in a soluble form. It has to be noted that collagen in fibres is bound to surrounding molecules by chemical crosslinks, which can induce an additive stabilising effect. Such an effect is not accounted for in the polymer in a box model, even if it is still unclear whether there is a relationship between box lateral dimension and degree of crosslinking or not. Soluble collagen does not possess such crosslinks and then can denature more easily, involving a lower amount of thermal energy. If the concentration of “soluble” collagen is enough high, the endothermic peak pattern becomes “bimodal”, with the two peaks representing the two different populations of collagens. As an example, sample C is characterised by a relatively low linear modulus value and shrinkage temperature as well (see Fig. 4, blue line). This leads us to assume that this sample represents immature tissue, and this is confirmed by the DSC diagram, in which the two different populations of collagen are present. The DSC thermogram of bovine skin supports this hypothesis: in this case, denaturation peaks are more regularly shaped.

Hydrothermal isometric tension can provide useful information on the type of crosslinks present in the dermis by measuring their thermal stability. During the HIT test the stress source is mainly collagen triple helix unwinding. During shrinking, individual collagen molecules transfer the stress to the surrounding molecules via chemical covalent crosslinks. In natural tissues, a broad spectrum of crosslinks exists. Each type of crosslink is characterised by a certain thermal stability. For this reason, heat labile crosslinks could break down as the temperature increases, causing the denatured network to relax. Changes in stress signal are thus the result of two competitive factors: denaturation of triple helices and break down of the dentatured network.

The HIT plot of adult tissue differs significantly from the foetal one. The latter exhibits a maximum, which suggests that foetal collagen molecules are mainly crosslinked with heat labile crosslinks.

Interesting results can be gathered by overlapping the HIT curve with the DSC thermogram.

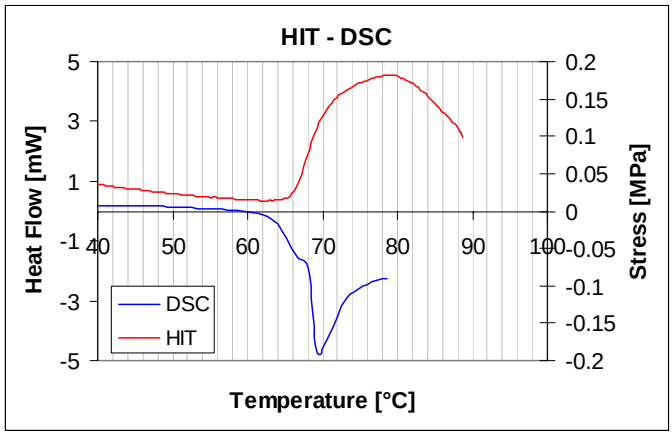

Fig. 20 Sample U HIT – DSC profiles comparison

As far as foetal tissue are concerned, it seems that DSC instrument starts to record collagen denaturation slightly earlier than HIT. This observation is consistent with the hypothesis of the presence of two different populations of collagen molecules in the foetal tissue, i.e. the soluble one which is not constrained by chemical crosslinks, denatures at relatively low temperatures, but since it is not linked to the surrounding molecules, it does not transfer any load and then the HIT does not record any signal. This is represented in the DSC thermogram by an early shoulder. The stress starts to increase significantly when the DSC thermogram becomes steeper. At this point the DSC equipment has to supply higher thermal power in order to denature the crosslinked collagen and up to this point the dominating factor is the uncoiling of crosslinked collagen. After that relaxation phenomena become to be more significant. The DSC peak then represents the temperature at which thermally labile crosslinks start to break and in correspondence to the peak, the HIT exhibits a slight change in slope, which reflects that relaxation phenomena beginning to occur. After this rupture, collagen molecules are unconstrained and less energy is required for their uncoiling. This is shown in the DSC profile by a late shoulder after the peak; and in the HIT curve by a shallower curve. The HIT profile of mature skin is markedly different.

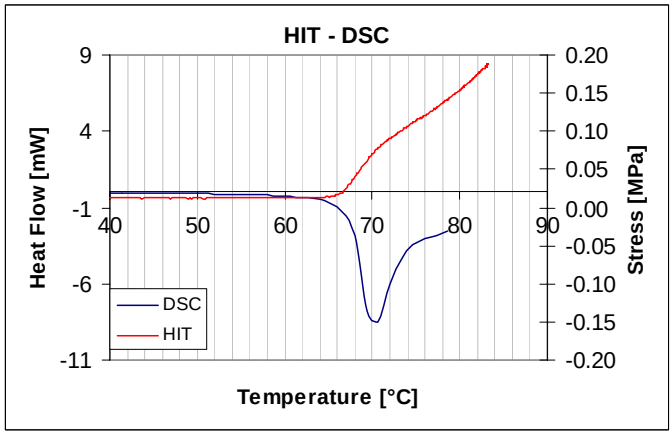

Fig. 21 Bovine skin HIT – DSC profile comparisons

Sample shrinking roughly starts at the same temperature recorded by the DSC, which accounts for protein denaturation. Moreover, the DSC profile is more symmetrical and regularly shaped, suggesting that mature skin is practically devoid of heat labile crosslinks. Nevertheless, a late shoulder is present. In this case, the presence of such a shoulder ought to

be ascribed to a protection mechanism, due to the existence of heat stable crosslinks which prevent the triple helices unwinding.

Starting from these observations, a linear modulus dependence on the shrinkage temperature has been found, as shown in Fig. 22

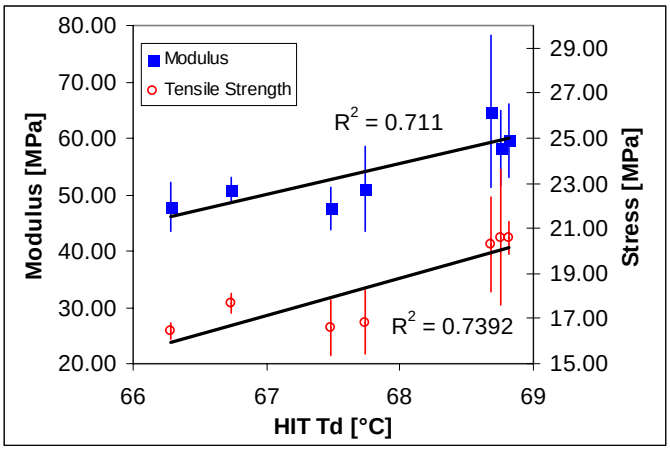

Fig. 22 Modulus (solid squares) and tensile strength (hollow circles) vs shrinkage temperature

Foetal skins with higher shrinkage temperature possess higher crosslinking density. These crosslinks induce a stiffening effect on the collagen bundles stretching. In Fig. 22, the values of the linear modulus were reported as a function of the shrinkage temperature rather than the DSC onset temperature, since the latter is affected by the denaturation of no-load bearing collagen molecules.

In order to evaluate the activation energy involved in the relaxation process, a stepwise HIT was done. According to [11], stress relaxation in a denatured polymeric network can be described by equation 1

$$\frac{\sigma(t)}{\sigma(t_0)} = \frac{N_t}{N_0} = e^{-kt} \qquad \text{-1-}$$

provided that isothermal condition has been achieved. In particular $\sigma(t)$ is the stress at time t, while $\sigma(t_0)$ denotes the stress value when the isotherm is achieved, N_t is the total number of load bearing polymeric chains remaining per unit volume at time t and N_0 is the initial number of load bearing polymeric chains. k is the rate constant which is age dependent. It is here assumed that the rate constant k should vary according to an Arrhenius equation:

$$k = Ae^{-\frac{E_a}{RT}} \qquad \text{-2-}$$

where A is a pre-exponential constant, R the gas constant and the temperature T is expressed in Kelvin. The half time of stress decay is defined by the following equation:

$$\frac{\sigma(t_{1/2})}{\sigma(t_0)} = \frac{1}{2} = e^{-kt_{1/2}} \qquad \text{-3-}$$

hence

$$\ln\left(t_{1/2}\right) = C + \frac{E_a}{RT} \qquad \text{-4-}$$

where $C = \ln\left(0.693/A\right)$. E_a is the slope of the regression line of the $\ln\left(t_{1/2}\right)$ versus T^{-1} plot. Regression lines and E_a values are reported below.

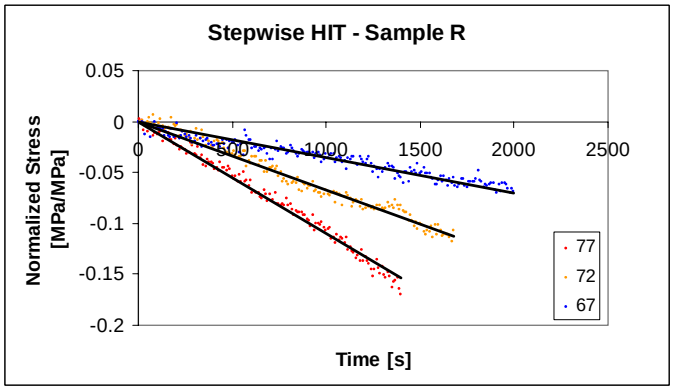

Fig. 23 Sample R Stepwise HIT regression lines

	Activation Energy [kcal/mol]	
	AVG	ST. DEV
R: step HIT	93.8	15.8

Table 9 Sample R activation energy values

The E_a value here reported is consistent with the results of previous works [13] and is comparable to the activation energy involved in peptide bond hydrolysis. However the half time of stress decay and the activation energy evaluated for the $NaBH_4$ treated tissues are much higher as shown in Fig. 24 and in Table 10.

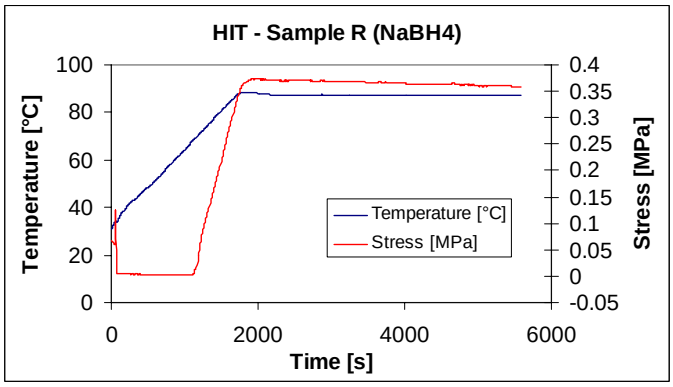

Fig. 24 Sample R ($NaBH_4$ treated) HIT profile

	K [s^{-1}]		half time [s]	
	AVG.	ST. DEV.	AVG.	ST. DEV.
R ($NaBH_4$)	0.000010	0.000001	70000	7000

Table 10 Sample R ($NaBH_4$ treated) HIT results

This suggests that the primary structure of the denatured collagen network, i.e. the α-chains, is unlikely to undergo peptide bond hydrolysis. Tissue thermal stability has to be ascribed to the presence of stable crosslinks.

Conclusions

The present work is an early attempt to determine a relationship between tissue composition, structure and physical properties. It is not, of course, an easy task owing to the strong heterogeneities which are present in the native tissue, in terms of composition and spatial arrangement of the microconstituents. As an example elastic network is mainly responsible for the early mechanical response of the tissue, but the effect of other interfibrillar components should not be neglected. In particular the interaction of the glycosaminoglycan reticulus with the ground substance, which wraps around the collagen bundles, could play important roles. Moreover, elastin is not spread uniformly throughout the thickness and its relative influence on grain should be higher than in the corium. Selective enzymatic removal of the ECM components should be carried out in order to assess the relative influences of the major constituents on the overall macroscopic properties.

ANNEX 1 - Preparation of leather from the salt foetal skin

Type of original material: Salted Friesian foetal skin

Process	Product	°C	%	Run	Remarks
Soak	Water	20	600	Run overnight	Sample collection
Flesh	Remove excess adipose tissue from the flesh side of the hide				
Lime	Water	20	200	1h	
	Na_2S		3		
	$Ca(OH)_2$		2	1h	
Wash	Water	20		10min and drain	
Delime	NH_4Cl	20	3.0	12h (in 20%water float)	pH= 8.5-9.0
Bate	Enzymes	37	0.1	1h and drain	
Wash	Water	20	200	10 min and drain	
Pickle	Water	20	100	24h	
	NaCl		20		Diluted 1:5
	H_2SO_4		1		Diluted 1:5 Sample collection
Chrome Tan	Chrome powder	30	8	Run overnight	
	MgO	45	0.4	4h	pH= 3.7
Drain , Horse overnight					
Neutralise	Water	25	200	30 min and drain	
	Water	40	100	1h and drain	pH= 6.2
	$NaHCO_3$		1.5		Diluted 1:5
Fatliquor	Water	50	50	2h	Diluited 1:4
	Sulphated oil		5		
	Sulphited oil		5		
	HCOOH	50		2h	pH= 3.5
Drain, toggle dry with no tension					
Condition					
Buff flesh side					

References

1. Jamall I.S., Finelli V.N., Que Hee S.S.: A simple method to determine nanogram levels of 4-hydroxyproline in biological tissues. *Analytical Biochemistry* 112, 70-75, 1981
2. Wright D.M., Attenburrow G.E.: The set and mechanical behaviour of partially processed leather dried under strain. *Journal of Materials Science* 35, 1353 – 1357, 2000.
3. Billiar K.L., Sacks M.S.: A method to quantify the fiber kinematics of planar tissues under biaxial stretch. *Journal of Biomechanics* 30, 753-756, 1997.
4. Hepworth D.G, Steven-Fountain A., Bruce D.M., Vincent J.F.V.: Affine versus non-affine deformation in soft biological tissues, measured by the reorientation and stretching of collagen fibres through the thickness of compressed porcine skin. *Journal of Biomechanics* 34, 341-346, 2001.
5. Boote C., Sturrock E.J., Attenburrow G.E., Meek K.M.: Pseudo-affine behaviour of collagen fibres during the uniaxial deformation of leather. *Journal of Materials Science* 37, 3651-3656, 2002.
6. Covington A.D., Song L.: Crosslinking – what crosslinking? *Leather International* October 2003.
7. Osaki S.: Distribution Map of Collagen Fiber Orientation in a Whole Calf Skin. *The Anatomical Record* 254, 147 – 152, 1999.
8. Fung Y.C.: Biomechanics: Mechanical properties of living tissues. *Ed. Springer* Chapter 7, 242-320, 1993.
9. Miles C.A., Bailey A.J.: Thermal Denaturation of Collagen Revisited. *Proceedings of the Indian Academy of Sciences*: Chemical Sciences. 111, 71-80, 1999.
10. Miles C.A., Ghelashvili M.: Polimer-in-a-Box Mechanism for the Thermal Stabilization of Collagen Molecules in Fibres. *Biophysical Journal* 76, 3243-3252, 1999.
11. Le Lous M., Allain J.-C., Cohen-Solal L., Maroteaux P. : The Rate Of Collagen Maturation in Rat and Human Skin. *Connective Tissue Research* 9, 253-262, 1982.
12. Allain J.C., Le Lous M., Bazin S., Bailey A.J., Delaunay A. : Isometric Tension Developed During Heating of Collagenous Tissues. *Biochimica et Biophysica Acta*. 533, 147-155, 1978.
13. Naimark, W. A., Waldman S. D., Anderson R. J., Suzuki B., Pereira C. A., Lee J. M.: Thermomechanical analysis of collagen crosslinking in the developing lamb pericardium. *Biorheology* 35, 1-16, 1998.
14. Le Lous M., Flandin F., Herbage D., Allain J.-C. : Influence of collagen denaturation on the chemorheological properties of skin, assessed by differential scanning calorimetry and hydrothermal isometric tension measurement. *Biochimica et Biophysica Acta* 717, 295 – 300, 1982.
15. Wright N.T., Humphrey J.D.: Denaturation of Collagen Via Heating: An Irreversible Rate Process**.** *Annual Review of Biomedical Engineering* 4, 109-128, 2002.